Supporting information

Tin porphyrin axially-coordinated two-dimensional covalent organic polymer for efficient hydrogen evolution

Qi Wang, Aijian Wang*, Yuqin Dou, Xiaoliang Shen, M. Shire Sudi, Long Zhao*, Weihua Zhu, Longhua Li*

School of Chemistry & Chemical Engineering, Jiangsu University, Zhenjiang 212013, P.R. China

Corresponding Author. Tel: +86-511-88791928. E-mail: wajujs@ujs.edu.cn, longzhao@ujs.edu.cn, longhuali@ujs.edu.cn

Experimental section

Reagents and materials

Tin(II) chloride ($SnCl_2$), Ni foam (NF), Nafion (5 wt%) and NaOH are obtained from Sinopharm Chemical Reagent Co., Ltd. All reagents and solvents are of chemical or analytical grade and were used without further purification. The deionized water was used throughout all the experiments including electrocatalytic processes. 5,10,15,20-Tetrakis(4-hydroxy-phenyl) porphyrin (TPP) and dichloro(5,10,15,20- tetraphenylporphyrinato)tin(IV) (SnTPP) were prepared based on previously reported methods with slight modifications.[1]

Material Characterizations

The morphologies, composition and structure of all samples were studied by the scanning electron microscopy (SEM, a Model S4800, Hitachi), X-ray photoelectron spectroscopy (XPS, a RBD upgraded PHI-5000C ESCA), Fourier-transform infrared (FTIR) spectra (a MB154S-FTIR spectrometer, Bomem, Canada), UV–Vis spectra recorded using a Varian Cary 500 spectrophotometer, and solid ^{13}C NMR spectra (a Bruker AVIII 400 MHz instrument using a BBFO probe). Density functional theory (DFT) calculations were performed with the Gaussian 09 program.

Electrochemical measurements

All electrochemical measurements including HER LSV curves were recorded on

a CHI 614E electrochemical workstation (CH Instrument, China) in 1.0 M KOH solution. The sample covered NF is used as the working electrode, a Pt gauze (1 × 1 cm^2) as the counter electrode and a mercury/ mercury oxide electrode (MOE) as the reference electrode. The long-term stability of SnTPPCOP was also studied by using the same electrolyzer. To prepare the working electrode, the catalysts (2 mg) and Nafion solution (5 wt%, 40 μL) were dispersed in CH_3CH_2OH (0.5 mL), then the solution was sonicated for 1.0 h to give the homogeneous ink. Subsequently, the well-mixed suspension (80 μL) was loaded onto the NF paper. The obtained electrode was then dried naturally at room temperature and retained for use. The measured potential in this work has been calibrated with the reversible hydrogen electrode potential (RHE) based on Nernst equations. The electrochemical impedance spectroscopy (EIS) measurement was recorded in the frequencies ranging from 0.01 Hz to 100 KHz with an amplitude of 1 mV. The double-layer capacitance of the as-synthesized samples is determined by the cyclic voltammograms with different scan rates (20, 40, 60, 80, and 100 mV/s) in the scope of 0-0.4 V *vs.* RHE.

The production of H_2 during a potentiostatic electrolysis experiment was determined by the water displacement method. If the initial height of water in the gas gathering tube before the gas gathering experiment is h_0, and after the potentiostatic electrolysis experiment the generated gas is gathered into the tube and the final height of water in the gas gathering tube become h_1, then the volume of generated gas (V) should be $s(h_0-h_1)$, where s is the inner cross-sectional area of the gas gathering tube. At the initial status, the pressure inside the gas gathering tube (P_0) is $P - \rho g h_0$, where P is the atmospheric pressure, ρ is the density of water, and g is the acceleration due to gravity. The output voltage of the differential pressure transducer would be $U_0 = k(P - P_0) = k\rho g h_0$, where k is the sensitivity of the differential pressure transducer (1 mV/Pa for a Freescale MPXV7002DP). When the height of water in the gas gathering tube decreases to h_1, the pressure inside the gas gathering tube becomes P_1, and $P_1 = P - \rho g h_1$. Then, the output of the differential pressure transducer is $U_1 = k(P - P_1) = k\rho_g h_1$. Accordingly, the volume of generated gas can be computed by $V = s(h_0 - h_1) = s(U_0/k\rho_g - U_1/k\rho_g) = s(U_0 - U_1)/k\rho_g = C(U_0 - U_1)$, where C is a coefficient that can be

calibrated by injecting a known volume of gas into the gas gathering tube and recording the variation of output voltage of the differential pressure transducer.

Preparation of SnTPPCOP

The novel tin porphyrin axially-coordinated 2D covalent organic polymer (SnTPPCOP) was prepared via a straightforward nucleophilic substitution (Scheme 1). In a typical synthetic route, SnTPP (0.02 mol) and TPP (0.01 mol) were added into a mixture of anhydrous tetrahydrofuran (50 mL) and pyridine (20 mL). And then the homogeneous solution was heated under flux for 5 days. The resultant solution was allowed to cool to room temperature and then was diluted with CH_3OH. The precipitate was collected by filtration through a 0.45 μm nylon membrane. The obtained filter cake was washed with water, anhydrous tetrahydrofuran and CH_3OH for several times to remove byproducts until the filtrate became colorless. Then, the powder was dried at room temperature under vacuum for 6 h to afford the desired SnTPPCOP.

Kinetic analysis based on the dual-pathway kinetic model

We performed kinetic analyses to evaluate thestandard activation free energies for the three elementary reaction steps of HER following the procedure of Wang et al.[2,3] and Hu et. al.[4] There are three elementary reaction steps for the alkaline HER on the catalysts' surfaces, including Volmer step ($H_2O + e^- \rightarrow H_{ad} + OH^-$), Heyrovsky step ($H_2O + H_{ad} + e^- \rightarrow H_2 + OH^-$) and Tafel step ($2H_{ad} \rightarrow H_2$). Under steady-state conditions, $d\Theta/dt = v_T + v_H - v_V = 0$ ($v_T + v_H = v_V$), where v is the reaction rate, and Θ is the surface coverage of the active reaction intermediate. The current is directly proportional to the sum of the reaction rates for the two single electron-transfer reactions ($j_i = 2Fv_i$). Thus, the total kinetic currents (j_k) can be expressed as below:

$$\begin{aligned} j_k &= F(v_V + v_H) = (j_V + j_H)/2 \\ &= 2F(v_T + v_H) = j_T + j_H \\ &= 2F(v_V - v_T) = j_V - j_T \end{aligned} \quad \text{(S1)}$$

The kinetic currents for each individual step are:

$$j_T = j * e^{-\triangle G^{*0}_{+T}/kT}[(1-\theta)^2 - e^{2\triangle G^{0}_{ad}/kT}\theta^2] \quad \text{(S2)}$$

$$j_H = j * e^{-\triangle G^{*0}_{+H}/kT}[e^{0.5\eta/kT}(1-\theta) - e^{(\triangle G^{0}_{ad} - 0.5\eta)/kT}\theta] \quad \text{(S3)}$$

$$j_V = j * e^{-\triangle G^{*0}_{-V}/kT}[e^{(\triangle G^{0}_{ad} + 0.5\eta)/kT}\theta - e^{-0.5\eta/kT}(1-\theta)] \quad \text{(S4)}$$

where ΔG represents the free energies of Volmer step ($\triangle G^{*0}_{-V}$), Heyrovsky step ($\triangle G^{*0}_{H}$), Tafel step ($\triangle G^{*0}_{T}$) and H*adsorption ($\triangle G^{0}_{ad}$).

The calculation of the adsorption isotherm (Θ) is given as below:

$$\Theta = \frac{-B - \sqrt{B^2 - 4AC}}{2A} \quad \text{(S5)}$$

$$A = 2T_p - 2T_m \quad \text{(S6)}$$

$$B = -4T_p - H_p - H_m - V_p - V_m \quad \text{(S7)}$$

$$C = 2T_p + H_p + V_m \quad \text{(S8)}$$

$$T_p = e^{-\triangle G^{*0}_{+T}/kT} \quad \text{(S9)}$$

$$T_m = e^{-(\triangle G^{*0}_{+T} + 2\triangle G^{0}_{ad}/kT} \quad \text{(S10)}$$

$$H_p = e^{-(\triangle G^{*0}_{+H} - 0.5\eta)/kT} \quad \text{(S11)}$$

$$H_m = e^{-(\triangle G^{*0}_{+H} - \triangle G^{0}_{ad} + 0.5\eta)/kT} \quad \text{(S12)}$$

$$V_p = e^{-(\triangle G^{*0}_{-V} - \triangle G^{0}_{ad} - 0.5\eta)/kT} \quad \text{(S13)}$$

$$V_m = e^{-(\triangle G^{*0}_{-V} + 0.5\eta)/kT} \quad \text{(S14)}$$

The kT is 25.51 meV at 300 K. The kinetic current, $j_k(\eta) = f(\triangle G^{*0}_{-V}, \triangle G^{*0}_{+H}, \triangle G^{*0}_{+T}, \triangle G^{0}_{ad}, j, \theta)$ can be determined by equations of S1-S4, in which the adsorption isotherm, $\Theta(\eta) = f(\triangle G^{*0}_{-V}, \triangle G^{*0}_{+H}, \triangle G^{*0}_{+T}, \triangle G^{0}_{ad})$ can be obtained from equations of S5-S14.

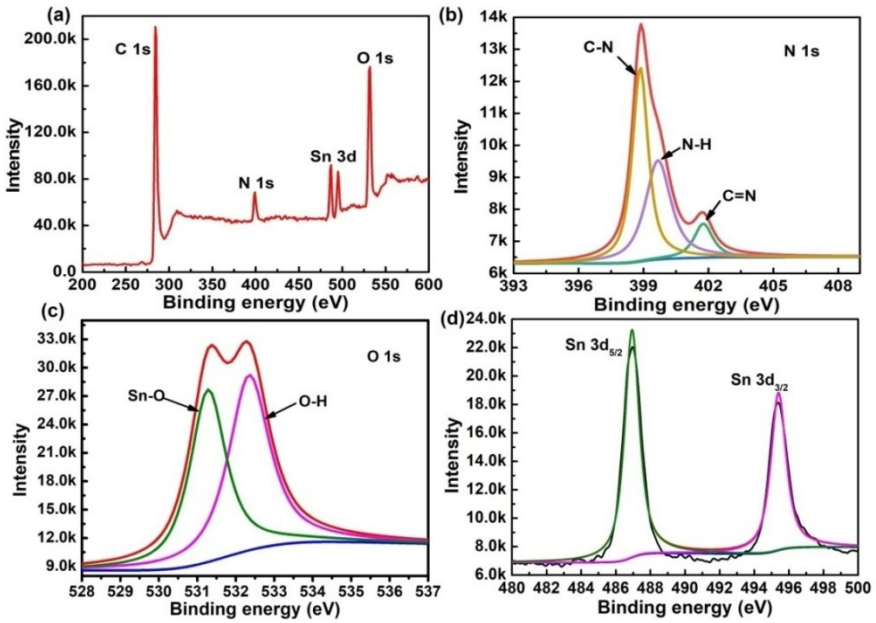

Figure S1. (a) XPS survey spectrum of SnTPPCOP; High-resolution XPS spectra of (b) N 1s, (c) O 1s and (d) Sn 3d.

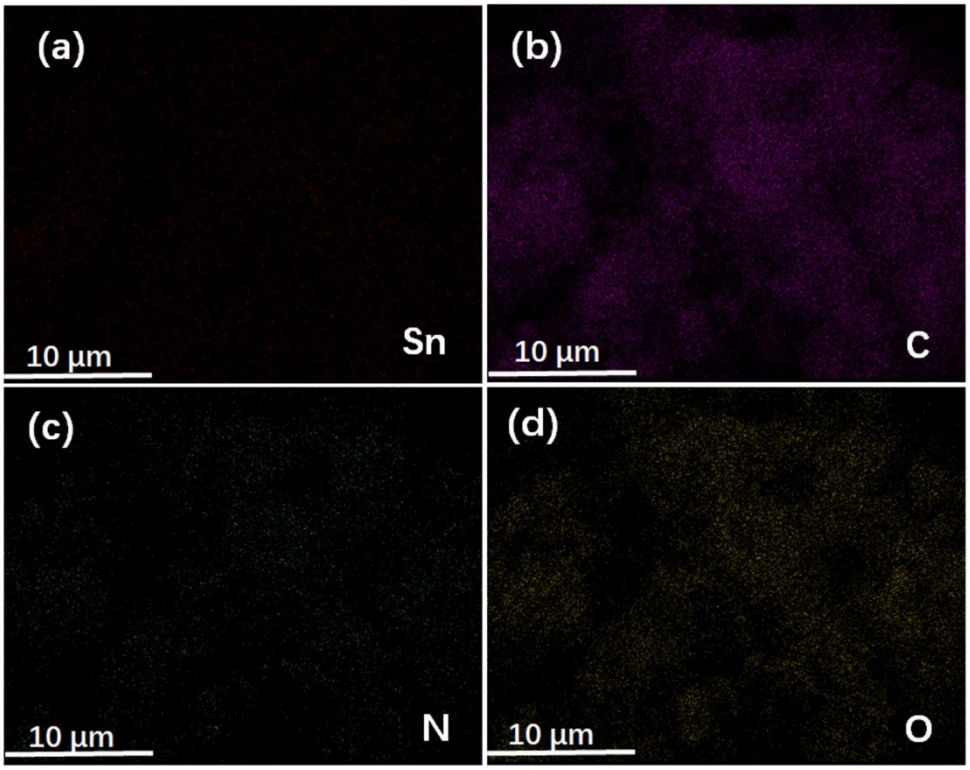

Figure S2. The merged elemental mapping images of SnTPPCOP.

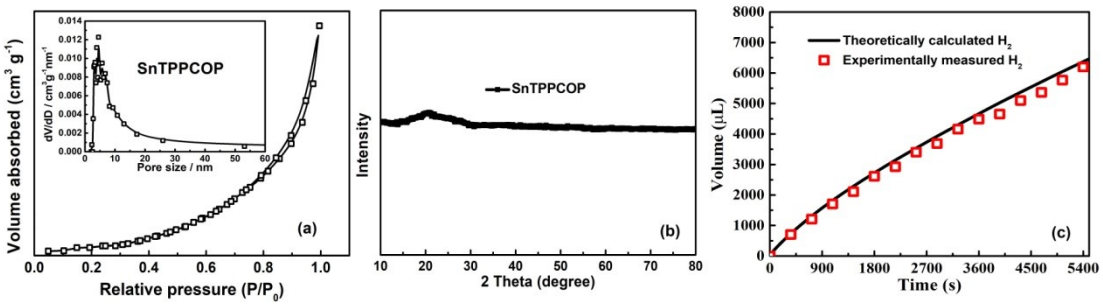

Figure S3. (a) The nitrogen adsorption-desorption isotherms (Insert is the pore width distribution curve), (b) XRD pattern and (c) the amount of H_2 experimentally measured and theoretically calculated as a function of time for SnTPPCOP.

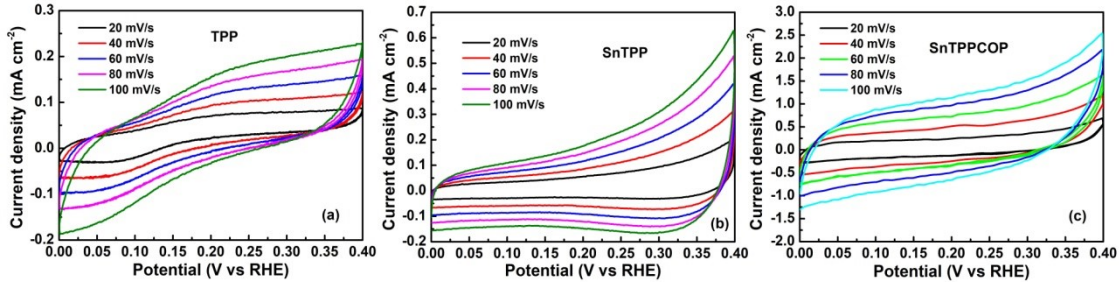

Figure S4. CV measurements with various scan rates for (a) TPP, (b) SnTPP and (c) SnTPPCOP.

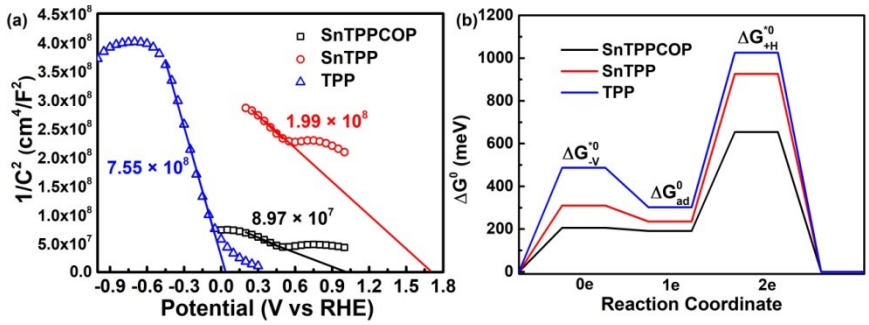

Figure S5. (a) Mott-Schottky plots and (b) free energy diagram of the as-prepared samples.

Table S1. Comparison of HER performance of SnTPPCOP with some other reported electrocatalysts.

Electrocatalysts	Overpotential (mV@10 mA cm^{-2})	Ref.
CoS_2/CoSe@C	164 (1.0 M KOH)	5
$Co_{0.9}Ni_{0.1}Se$	186 (1.0 M KOH)	6
CoSe@NCNT/NCN	197 (0.5 M H_2SO_4)	7
$NiSe_2$@N-doped carbon	162 (1.0 M KOH)	8
$NiSe_2$@NG	201 (0.5 M H_2SO_4)	9
Co_9S_8@MoS_2	239 (1.0 M KOH)	10
FeMoP-0.10	195 (1.0 M KOH)	11
MoP NTs/Mo	269 (1.0 M KOH)	12
MoP@NCF	234.6 (0.5 M H_2SO_4)	13
CoP(MoP)-$CoMoO_3$@CN	198 (1.0 M KOH)	14
TiCP-PCP	339 (0.5 M H_2SO_4)	15
SB-PORPy-COF	380 (η_5, 0.5 M H_2SO_4)	16
CoTCPP polymer	475 (0.5 M H_2SO_4)	17
CoOx-N-C/TiO_2C(22.7%)	367.8 (1.0 M KOH)	18
Cu-CMP700	350 (1.0 M KOH)	19
CoP-nph-CMP-800	360 (1.0 M KOH)	20
CoCOP	310 (1.0 M KOH)	21
COF-$Ni(OH)_2$	258 (1.0 M KOH)	22
Ru@COF-1	200 (0.5 M H_2SO_4)	23
C6-TRZ-TFP COF	200 (0.5 M H_2SO_4)	24
THTNi 2DSP	330 (0.5 M H_2SO_4)	25
SnTPPCOP	**147**	**This work**

References

[1] V.S. Shetti, M. Ravikanth, Sn(IV) porphyrin based axial-bonding type porphyrin triads containing heteroporphyrins as axial ligands, Inorg. Chem. 49 (2010) 2692-2700.

[2] J.X. Wang, T.E. Springer, P. Liu, M. Shao, R.R. Adzic, Hydrogen oxidation reaction on Pt in acidic media: Adsorption isotherm and activation free energies. J. Phys. Chem. C 111 (2007) 12425-12433.

[3] J.X. Wang, T.E. Springer, R.R. Adzic, Dual-pathway kinetic equation for the hydrogen oxidation reaction on Pt electrodes. J. Electrochem. Soc. 153 (2006) A1732.

[4] J. Hu, C. Zhang, L. Jiang, H. Lin, Y. An, D. Zhou, M.K.H. Leung, S. Yang, Nanohybridization of MoS_2 with layered double hydroxides efficiently synergizes the hydrogen evolution in alkaline media. Joule 2017,1, 383-393.

[5] K. Karuppasamy. R. Bose, V.R. Jothi, D. Vikraman, Y.T. Jeong, P. Arunkumar, D.B. Velusamy, T. Maiyalagan, A. Alfantazi, H.S. Kim, High performance, 3D-hierarchical CoS_2/CoSe@C nanohybrid as an efficient electrocatalyst for hydrogen evolution reaction, J. Alloys Compd. 838 (2020) 155537.
[6] W.W. Zhong, Z.P. Wang, N. Gao, L.G. Huang, Z.P. Lin, Y.P. Liu, F.Q. Meng, J. Deng, S.F. Jin, Q.H. Zhang, L. Gu, Coupled vacancy pairs in Ni-doped CoSe for improved electrocatalytic hydrogen production through topochemical deintercalation, Angew. Chem. Int. Ed. 59 (2020) 22743-22748.
[7] M. Yang, Y.Y. Yang, K.Z. Wang, S.W. Li, F. Feng, K. Lan, P.B. Jiang, X.K. Huang, H.L. Yang, R. Li, Facile synthesis of CoSe nanoparticles encapsulated in N-doped carbon nanotubes-grafted N-doped carbon nanosheets for water splitting, Electrochimica Acta 337 (2020) 135685.
[8] Z.D. Huang, S. Yuan, T.T. Zhang, B. Cai, B. Xu, X.Q. Lu, L.L. Fan, F.N. Dai, D.F. Sun, Selective selenization of mixed-linker Ni-MOFs: $NiSe_2$@NC core-shell nanooctahedrons with tunable interfacial electronic structure for hydrogen evolution reaction, Appl. Catal. B: Environ. 272 (2020) 118976.
[9] W.X. Li, B. Yu, Y. Hu, X.Q. Wang, D.X. Yang, Y.F. Chen, Core-shell structure of $NiSe_2$ nanoparticles@nitrogen-doped graphene for hydrogen evolution reaction in both acidic and alkaline media, ACS Sustaniable Chem. Eng. 7 (2019) 4351-4359.
[10] L.H. He, S.J. Huang, Y.K. Liu, M.H. Wang, B.B. Cui, S.D. Wu, J.M. Liu, Z.H. Zhang, M. Du, Multicomponent Co_9S_8@MoS_2 nanohybrids as a novel trifunctional electrocatalyst for efficient methanol electrooxidation and overall water splitting, J. Colloid Interf. Sci. 586 (2021) 538-550.
[11] X. Liang, D. Z. Zhang, Z. Z. Wu, D. Z. Wang, The Fe-promoted MoP catalyst with high activity for water splitting, Appl. Catal. A: Gen. 524 (2016) 134-138.
[12] H.N. Yu, S. Cao, B. Fu, Z. J. Wu, J. J. Liu, L. Y. Piao, Self-supported nanotubular MoP electrode for highly efficient hydrogen evolution via water splitting, Catal. Commun. 127 (2019) 1-4.
[13] J. S. Li, J. Y. Li, X. R. Wang, S. Zhang, J. Q. Sha, G. D. Liu, Reduced graphene oxide-supported MoP@P-doped porous carbon nano-octahedrons as high-performance electrocatalysts for hydrogen evolution, ACS Sustainable Chem. Eng. 6 (2018) 10252-10259.
[14] L. Yu, Y. Xiao, C. L. Luan, J. T. Yang, H. Y. Qiao, Y. Wang, X. Zhang, X. P. Dai, Y. Yang, H. H. Zhao, Cobalt/molybdenum phosphide and oxide heterostructures encapsulated in N-doped carbon nanocomposite for overall water splitting in alkaline media, ACS Appl. Mater. Interfaces 11 (2019) 6890-6899.
[15] A.J. Wang, L.X. Cheng, X.L. Shen, W.H. Zhu, L.H. Li, Mechanistic insight on porphyrin based porous titanium coordination polymer as efficient bifunctional electrocatalyst for hydrogen and oxygen evolution reactions, Dyes Pigments 181 (2020) 108568.
[16] S. Bhunia, S. K. Das, R. Jana, S. C. Peter, S. Bhattacharya, M. Addicoat, A. Bhaumik, A. Pradhan, Electrochemical stimuli-driven facile metal-free hydrogen evolution from pyrene-porphyrin-based crystalline covalent organic framework, ACS Appl. Mater. Interfaces 2017, 9, 23843-23851.
[17] Y. Y. Wu, J. M. Veleta, D. Tang, A. D. Price, C. E. Botez, D. Villagran, Efficient

electrocatalytic hydrogen gas evolution by a cobalt-porphyrin-based crystalline polymer, Dalton Tans. 2018, 47, 8801-8806.

[18] L. H. He, J. M. Liu, B. Hu, Y. K. Liu, B. B. Cui, D. L. Peng, Z. H. Zhang, S. D. Wu, B. Z. Liu, Cobalt oxide doped with titanium dioxide and embedded with carbon nanotubes and graphene-like nanosheets for efficient trifunctional electrocatalyst of hydrogen evolution, oxygen reduction, and oxygen evolution reaction, J. Power Soures 2019, 414, 333-344.

[19] S. S. Cui, M. M. Qian, X. Liu, Z. J. Sun, P. W. Du, A copper porphyrin-based conjugated mesoporous polymer-derived bifunctional electrocatalysts for hydrogen and oxygen evolution, ChemSusChem 2016, 8, 2365-2373.

[20] H. X. Jia, Y. C. Yao, Y. Y. Gao, D. P. Lu, P. W. Du, Pyrolyzed cobalt porphyrin-based conjugated mesoporous polymers as bifunctional catalysts for hydrogen production and oxygen evolution in water, Chem. Commun. 2016, 52, 13483-13486.

[21] A.J. Wang, L.X. Cheng, W. Zhao, X.L. Shen, W.H. Zhu, Electrochemical hydrogen and oxygen evolution reactions from a cobalt-porphyrin-based covalent organic polymer, J. Colloidal Interf. Sci. 2020, 579, 598-606.

[22] D. Mullangi, V. Dhavale, S. Shalini, S. Nandi, S. Collins, T. Woo, S. Kurungot, R. Vaidhyanathan, Low-overpotential electrocatalytic water splitting with noble-metal-free nanoparticles supported in a sp^3 N-rich flexible COF, Adv. Energy Mater. 2016, 1600110.

[23] Y.X. Zhao, Y. Liang, D.X. Wu, H. Tian, T. Xia, W.X. Wang, W.Y. Xie, X.M. Hu, X.L. Tian, Q. Chen, Ruthenium complex of sp^2 carbon-conjugated covalent organic frameworks as an efficient electrocatalyst for hydrogen evolution, Small 2022, 2107750.

[24] S. Ruidas, B. Mohanty, P. Bhanja, E.S. Erakulan, R. Thapa, P. Das, A. Chowdhury, S.K. Mandal, B.K. Jena, A. Bhaumik, Metal-free triazine-based 2D covalent organic framework for efficient H_2 evolution by electrochemical water splitting, ChemSusChem 2021, 14, 5057-5064.

[25] X.L. Feng, M. Pfeffermann, H.W. Liang, Z.K. Zheng, X. Zhu, J. Zhang, X.L. Feng, Large-area, free-standing, two-dimensional supramolecular polymer single-layer sheets for highly efficient electrocatalytic hydrogen evolution, Angew. Chem. Int. Ed. 2015, 54, 12058-12063.